ARTICLE

Charge Mobility and Recombination in a New Hole Transporting Polymer and Its Photovoltaic Blend

Mein Jin Tan,[†] Wei-Peng Goh,[†] Jun Li,[†] Gaurav Pundir,[§] Vijila Chellappan,*[,†] and Zhi-Kuan Chen*[,†]

Institute of Materials Research and Engineering, ASTAR (Agency for Science, Technology and Research), 3 Research Link, Singapore 117602, and Department of Mechanical Engineering, National University of Singapore, 9 Engineering Drive 1, Singapore 117576

ABSTRACT The charge mobility in a new hole transporting polymer, poly(2,6-bis(thiophene-2-yl)-3,5-dipentadecyldithieno[3,2-b;2′,3′-d]thiophene) (PBTDTT-15), and its blend with (6,6)-phenyl-C_{70}-butyric acid methyl ester ($PC_{70}BM$) in a weight ratio of 1:3 at ambient atmosphere condition was investigated using time-of-flight (TOF) photoconductivity and photoinduced charge extraction by linearly increasing voltage (PhotoCELIV) techniques. The bulk heterojunction based photovoltaic (PV) blend (PBTDTT-15:$PC_{70}BM$ (1:3)) exhibited a promising power conversion efficiency (PCE) of 3.23% under air mass 1.5 global (AM 1.5G) illumination of 100mW/cm^2. The charge mobility and recombination properties of the best performing cells were investigated. The hole mobility in the pure PBTDTT-15 was in the range of 4×10^{-4} cm^2/(V s), which was reduced almost 5 times in the PBTDTT-15:$PC_{70}BM$ (1:3) blend. The PhotoCELIV transient observed for the photovoltaic (PV) blend was dominated by electrons, with the charge mobility of the order of 10^{-3} cm^2/(V s), and a weak shoulder at a long time scale due to holes. The effective bimolecular recombination coefficient (β) obtained for the PV blend deviated significantly from the Langevin recombination coefficient (β_L) indicating a phase-separated morphology. The obtained results indicate that the PBTDTT-15:$PC_{70}BM$ blend can be potential for organic solar cell applications.

KEYWORDS: polymeric solar cells • charge transport and recombination • PhotoCELIV • time of flight photoconductivity

1. INTRODUCTION

Research on π-conjugated materials have increased in recent years due to its solution processability, providing the potential for low cost fabrication in various optoelectronic applications such as photovoltaics (1), light emitting diodes (2, 3), and field-effect transistors (4, 5). Photovoltaic cells of a blend of π-conjugated polymers and fullerene derivatives have attracted significant research interest as the efficiency of bulk heterojunction (BHJ)-based polymer solar cells are making impressive improvements in the recent years (6−11). The most commonly used polymer solar cells consists of Poly(3-hexylthiophene):[6,6]-phenyl C_{60}-butyric acid methyl ester (P3HT:PCBM) and gives a power conversion efficiency (PCE) of around 5% (9). However, the energy conversion efficiency and stability of the polymeric solar cells needs to be considerably improved for these solar cells to be considered for practical applications. As a result, extensive synthesis efforts have been devoted in order to design new conjugated polymers with low band gaps to absorb the portion of the solar energy spectrum with the highest flux and to improve the air stability. Yu et al. (11) have demonstrated a polymer solar cell with PCE of ∼5.6% using a new semiconducting copolymer consists of alternating thieno-[3,4-b]thiophene and benzodithiophene (PTB1) blended with $PC_{70}BM$. Recently, Park et al. (11) have shown a promising solar cell efficiency of 6.1% using poly[N-9″-hepta-decanyl-2,7-carbazole-alt-5,5-(4′,7′-di-2-thienyl-2′,1′,3′-benzothiadiazole (PCDTBT) and $PC_{70}BM$ composite (12). In addition to the development of new low band-gap polymers, it has been shown that the efficiency of polymer solar cell can also be enhanced by stacking one or more solar cells with nonoverlapping spectral response in order to cover the broader solar spectrum compared to the single junction cells (13). Although, the device performance of different new polymers have been evaluated by various research groups, the charge transport properties of those new polymers and its BHJ photovoltaic blend are not investigated in detail. Charge transport is one of the major parameters affecting the device efficiency and stability of polymer solar cells. The charge-transport properties of the well-established organic photovoltaic blends such as P3HT:PCBM and MDMO-PPV:PCBM have already been investigated by Pivirikas et al. (14) and Mozer et al. (15) using photoinduced charge extraction by linearly increasing voltage (PhotoCELIV) technique. It has been shown that the photovoltaic characteristics in well-optimized devices are not limited by the charge transport or recombination as the electron and hole mobilities are highly balanced. However, the situation may be different in new photovoltaic blends containing new electron donors or electron acceptors, and thus it is important to investigate the

* Corresponding author. E-mail: c-vijila@imre.a-star.edu.sg (V.C.); zk-chen@imre.a-star.edu.sg (Z.-K.C.).

Received for review January 29, 2010 and accepted April 13, 2010

[†] Agency for Science, Technology and Research.

[§] National University of Singapore.

DOI: 10.1021/am100078g

Published on Web 04/23/2010

charge transport properties in order to maximize the device performances of those new PV layers.

In this paper, we report a new thiophene and dithienothiophene based hole transporting polymer: poly(2,6-bis-(thiophene-2-yl)-3,5-dipentadecyldithieno[3,2-b;2′,3′-d]thiophene) (PBTDTT-15) and its photovoltaic properties in a blend of PBTDTT-15:$PC_{70}BM$ (1:3). Polymers based on dithienothiophene (DTT), a sulfur and electron rich building block, have been attracting a lot of interest (16). DTT derivatives have been applied to optoelectronic applications such as organic thin film transistors (OTFT) (17, 18), as well as OPV and hybrid solar cells (19, 20), thus confirming its vast potential. Power conversion efficiency (PCE) for DTT derivative based PSCs so far have reached 1.40% for this class of materials (21). Insertion of DTT units to a polythiophene backbone yield polymers that have lower HOMO energy levels with respect to polyalkylthiophene, conferring better stability in ambient conditions (12). In this study, we observed a PCE of 3.23% for the newly synthesized PBTDTT-15 polymer blended with $PC_{70}BM$ using a simple device architecture of glass/ITO/PEDOT:PSS(40 nm)/PBTDTT-15:$PC_{70}BM$ (1:3) (300 nm)/Al (100 nm). The obtained device results indicate that this photovoltaic blend may be a potential candidate for solar cell applications as it showed promising PCE and air stability. Therefore, the charge transport properties of this photoactive layer of similar composition were investigated. There is no known report on charge transport properties of DTT derivatives and its copolymers. The charge transport properties in photovoltaic blends can be successfully investigated using PhotoCELIV technique; however, it is difficult to distinguish the sign of the carriers measured using PhotoCELIV. Therefore, we used both PhotoCELIV and time-of-flight (TOF) photoconductivity techniques in order to obtain the electron and hole mobility in the pure polymer and its photovoltaic blend. The effect of charge mobility and charge recombination properties on the density of photocharges were also studied and discussed in detail.

2. EXPERIMENTAL SECTION

The new hole transporting polymer: poly(2,6-bis(thiophene-2-yl)-3,5-dipentadecyldithieno[3,2-b;2′,3′-d] thiophene) (PBTDTT-15) with high molecular weight has been synthesized by the Stille coupling polymerization in chlorobenzene with tris(dibenzylideneacetone)dipalladium and tri(o-toyl)phosphine as catalyst system. The molecular weight of the PBTDTT-15 was estimated by gel-permeation chromatography (GPC) analysis in a THF solution relative to polystyrene standards. The number average molecular weight (M_n) was 80 000 with a polydispersity index (M_w/M_n) of 5. The electrochemical properties of the resulting polymers were studied by cyclic voltammetry (CV) with a three-electrode cell in a 0.1 M solution of tetrabutylammonium hexafluorophosphate (Bu_4NPF_6) in CH_3CN. The highest occupied molecular orbital (HOMO) level, calculated from the onset of the oxidation potentials obtained from CV curve of the polymer film, was 5.05 eV, about 0.15 eV larger than that of regioregular P3HT (4.9 eV) measured under the same conditions ensuring higher oxidative stability.

The newly synthesized PBTDTT-15 polymer was dissolved in 1,2-dichlorobenzene (DCB) solution at a concentration of 10 mg/mL. The chemical structure of the polymer is shown in Figure 1 (inset). Blends of PBTDTT-15 with $PC_{70}BM$ were prepared in

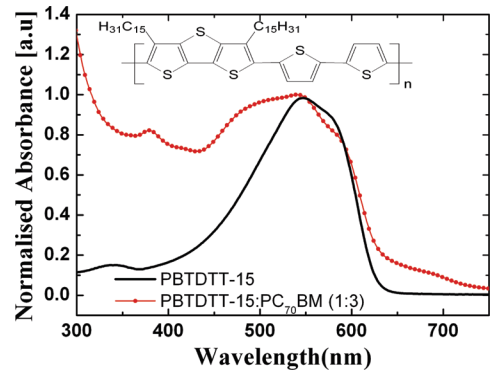

FIGURE 1. Absorbance spectrum of pure PBTDTT-15 and PBTDTT-15:$PC_{70}BM$ blend films; inset: the chemical structure of PBTDTT-15 polymer.

the concentration ratio of 1:3 in DCB. Fifteen microliters of 1,8-octanedithiol additive was mixed in 1 mL of PBTDTT-15:$PC_{70}BM$ to control the nanophase separation of the spin-coated film. $PC_{70}BM$ was selected as the n-type material because it has better light absorption in the visible region than PCBM. The patterned ITO glass substrates were first sonicated in a detergent bath for half an hour, followed by a rinsing of deionized water for 20 min. This was succeeded by sonicating in an acetone and isoproponal bath for 15 and 20 min, respectively. The cleaning step was concluded by drying the substrates in an oven at 80 °C for at least an hour. The substrates were subjected to an ozone plasma treatment for 10 min before a 40 nm thick PEDOT:PSS was spin-coated onto the ITO surface. The photoactive layer was spin-coated onto the PEDOT:PSS layer and left to dry for 2 h. A 100 nm thick aluminum was deposited onto the photoactive layer via thermal evaporation as the cathode. The active area of the device is 4 mm^2. Devices without PEDOT:PSS layer was used for charge transport studies.

The thickness of the films was measured using a surface profiler (KLA-Tencor P10 surface profiler). The absorbance measurements (UV−Vis) of the blend system were carried out using a Shimadzu UV-3101PC spectrophotometer. Current density−voltage ($J-V$) measurements were carried out in an inert environment (MBraun glovebox, N_2 atmosphere) under 1 Sun (AM1.5G) conditions using a solar simulator (SAN-EI Electric XES-301S 300W Xe Lamp JIS Class AAA) with an intensity of 100mW/cm^2.

The PhotoCELIV setup consists of a pulsed Nd:YAG laser, pulse generator, function generator and a digital oscilloscope. The sample was excited using the laser (pulse width <4 ns, pulse repetition rate 1 Hz) through the ITO side of the device. The photogenerated charge carriers were extracted using a linearly increasing voltage pulse of various amplitudes. The built-in field in the device was compensated by applying an offset voltage which is equivalent to the work function difference between the electrodes. The PhotoCELIV transients were recorded by varying the amplitudes of the voltage ramp, pulse widths and the time delay between the laser pulse and voltage pulse. The detailed photoCELIV measurement conditions were described somewhere else (22−24). The charge mobility and the density of photogenerated charge carriers were calculated from the time taken to reach the photocurrent maximum and the area of the photocurrent transients obtained from the transients. The charge recombination behaviors were also studied by varying the intensity of the laser and delay time between the laser pulse and the voltage pulse. The TOF photoconductivity measurements were carried out on thick films by generating the photocarriers at the ITO side of the device with simple device architecture of ITO/photoactive layer/Al. The light source used for the TOF experiment is a pulsed Nd:YAG laser; wavelength 532 nm; pulse width <4 ns, pulse repetition rate 1 Hz. The

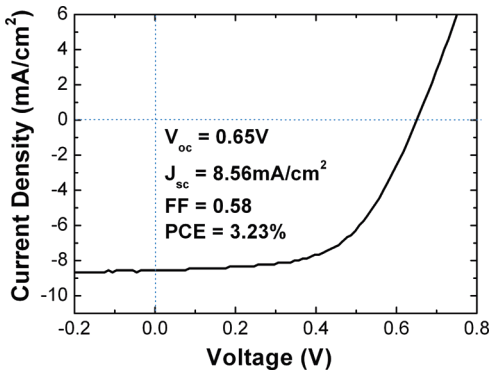

FIGURE 2. $J-V$ characteristics of a solar cell using PBTDTT-15: $PC_{70}BM$ (1:3) photoactive layer; the obtained device parameters are shown in the inset.

photocurrent under the influence of applied electric field was monitored across a variable resistor ($R = 50\ \Omega$ to 500Ω) using an oscilloscope. Care was taken to ensure that the time constant of the setup is less than the transit time ($RC < t_t$). The laser excitation intensity was adjusted in order to avoid the space charge effects. The experimental details of TOF photoconductivity setup can be found somewhere else (25, 26).

3. RESULTS AND DISCUSSION

3.1. Absorption Spectrum of Pure PBTDTT-15 and Its Blend with $PC_{70}BM$. The absorption spectrum of pure PBTDTT-15 and its blend with $PC_{70}BM$ is depicted in Figure 1. The chemical structure of PBTDTT-15 is shown in Figure 1 inset. The spectrum for pure PBTDTT-15 shows a peak at around 550 nm, with a shoulder at around 580 nm. The absorption range is between 400 to 630 nm. The absorption spectrum of PBTDTT-15:$PC_{70}BM$ is slightly red-shifted, thus aligning more toward the portion of the solar spectrum with higher flux compared to the P3HT: PCBM system.

3.2. Current Density−Voltage ($J-V$) Characteristics. The current density−voltage characteristics ($J-V$) of the solar cell with device architecture of glass/ITO/PEDOT:PSS(40 nm)/ PBTDTT-15:$PC_{70}BM$ (1:3) (300 nm)/Al (150 nm) was measured. In order to maintain the integrity of the devices, the characterization was performed in an inert (N_2) glovebox environment. The current density−voltage ($J-V$) graph is shown in Figure 2 and the photovoltaic parameters are summarized as an inset. The highest PCE of 3.23% was obtained for the devices annealed at 100 °C for 10 min. This is the highest PCE achieved so far for OPV devices based on DTT derivatives. The device efficiency may be increased further by optimizing the solvent evaporation rate and thickness of film. This confirms the potential of DTT derivatives for use in photovoltaic applications.

3.3. Charge Mobility in Pure PBTDTT-15. The charge mobility in pure PBTDTT-15 polymer layer of thickness 390 nm was calculated using the PhotoCELIV measurement on a device structure of ITO/PBTDTT-15(390 nm)/Al(150 nm). The PhotoCELIV transients for different amplitudes of linearly increasing voltage pulses with fixed pulse width (20 μs) were recorded and shown in Figure 3a. The time delay between the laser pulse and the voltage pulse was fixed at 20 μs. It can be seen that the time taken to reach the photocurrent maximum decreases with increasing the amplitude of voltage pulse, indicating the electric field dependence of charge mobility. The charge mobility was calculated using the moderately conducting case, in which the capacitor current is almost equal to the photocurrent within the photoactive layer (15). The calculated charge mobility was found to be 4.2×10^{-4} cm^2/(V s) at an applied electric field of 1.3×10^4 V/cm. The charge mobility was almost equal to the charge mobility reported for pure P3HT film which is around 4×10^{-4} cm^2/(V s) at similar applied electric fields (27). The charge mobility in a thick polymer film (4.45 μm) at room temperature was also studied using TOF photoconductivity (TOF) technique. The TOF transients for holes obtained for different applied voltages are shown in Figure 3b. The transit time was obtained from the log−log plot of the TOF transients (Figure 3b, inset) and calculated the charge mobility using the relation $\mu = d^2/Vt_T$, where d is the polymer film thickness, V is the applied voltage, and t_T is the transit time. The hole mobility in this polymer at ambient condition is 2.7×10^{-4} cm^2/(V s) at an applied electric field of 1.5×10^4 V/cm, which increased to 6×10^{-4} cm^2/(V s) at an applied electric field of 6.7×10^4 V/cm. The obtained charge mobility from the TOF and PhotoCELIV techniques (shown in Figure 4) using two different film thicknesses shows good agreement, indicating that the charge mobility was not affected by film morphology or thickness of the film.

3.4. Charge Mobility in the Photovoltaic Blend of PBTDTT-15 and $PC_{70}BM$. The charge transport properties of PBTDTT-15 blended with $PC_{70}BM$ in a ratio of 1:3 (w/w) (PBTDTT-15:$PC_{70}BM$) were also studied using PhotoCELIV and TOF technique. The film thickness used for this investigation was 700 nm. The PhotoCELIV transients for different amplitudes of voltage ramps are shown in Figure 4(a). The time taken to reach the photocurrent maximum decreased with an increase of the amplitude of voltage ramp. The calculated charge mobility was in the range of 3×10^{-3} cm^2/(V s), which is 1 order of magnitude higher than the charge (hole) mobility in the pure PBTDTT-15 layer. Therefore, the fast carrier mobility in the photovoltaic blend was assigned to electron mobility as the proportion of $PC_{70}BM$ in the blend is much higher than the polymer. It can also be seen that there is an additional shoulder in the PhotoCELIV transients at long times due to holes; however, the hole mobility value is difficult to calculate as the peak position is not clear. To identify the type of charge carrier in the photovoltaic blend, the TOF photoconductivity measurements were also carried out on the blend system. The TOF transients for electrons are shown in Figure 4b. The log−log plot of the electron transients are shown in Figure 4c. The electron and hole mobilities were obtained separately by changing the bias condition of the device. It was found that the electron and hole mobilities in the photovoltaic blend were around 3×10^{-3} cm^2/(V s) and 7.8×10^{-5} cm^2/(V s), respectively, at an applied electric field of 1.5×10^4 V/cm. The variation of charge mobility with applied electric field obtained from both PhotoCELIV and

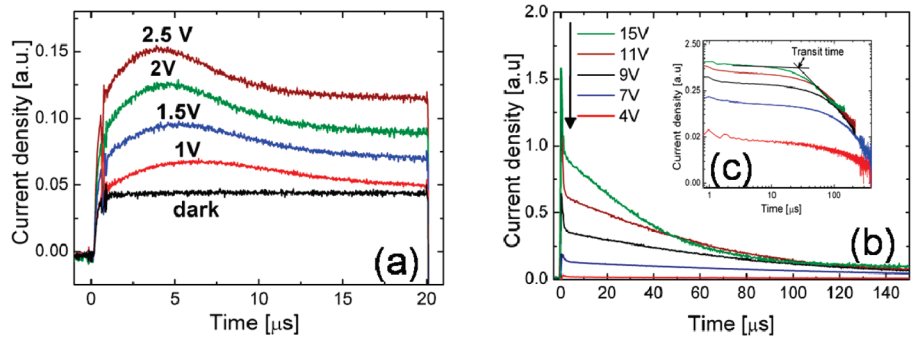

FIGURE 3. (a) PhotoCELIV transients recorded for pure PBTDTT-15 film of thickness 390 nm; (b) linear plot of time-of-flight hole transients measured for 4.45 μm thick PBTDTT-15 film; (c) inset shows the log−log plot of TOF hole transients.

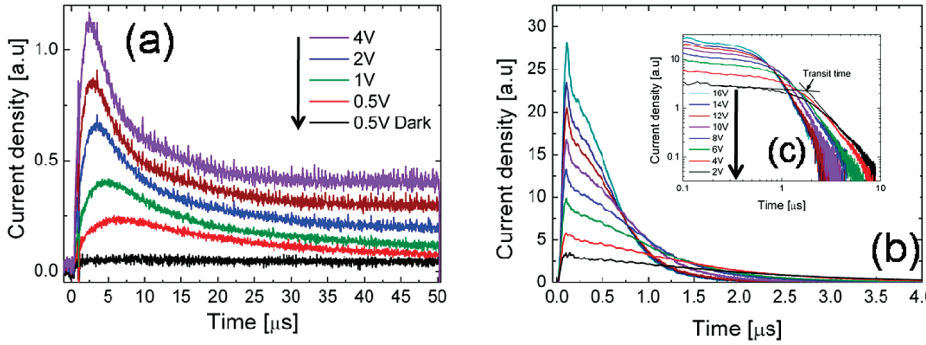

FIGURE 4. (a) PhotoCELIV transients recorded for PBTDTT-15:$PC_{70}BM$ (1:3) blend film of thickness 700 nm; (b) linear plot of time-of-flight hole transients measured for the same device; (c) Inset shows the log−log plot of TOF hole transients.

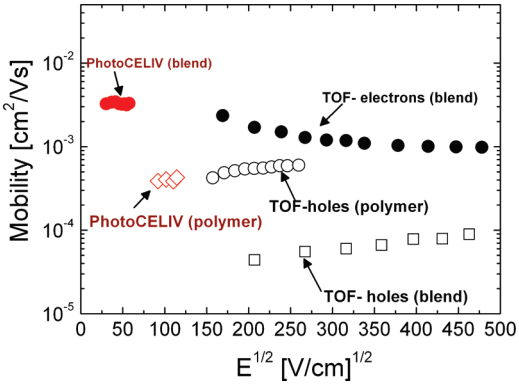

FIGURE 5. Electric field dependence of charge mobility in pure PBTDTT-15 film and PBTDTT-15:$PC_{70}BM$ (1:3) blend film obtained from PhotoCELIV and TOF-photoconductivity measurements.

TOF photoconductivity technique is shown in Figure 5. It can be seen that the charge mobility in the photovoltaic blend obtained by PhotoCELIV was close to the electron mobility obtained by TOF photoconductivity technique. In addition, the hole mobility in the photovoltaic blend was almost five times slower than the hole mobility in the pure polymer and this difference can be attributed to the change in film morphology with the addition of $PC_{70}BM$. The similar behavior has also been observed in poly[2-methoxy-5-(3,7-dimethyloctyloxy)-phenylenevinylene]:PCBM (MDMO-PPV:PCBM) blends, where the electron mobility is almost 2 orders of magnitude higher than the hole mobility measured using TOF photoconductivity technique (28).

3.5. Charge Recombination Studies in Pure PBTDTT-15 and Its Blend with $PC_{70}BM$. Charge recombination is one of the major parameters limiting the efficiency of the photovoltaic devices. Therefore the charge recombination behavior was investigated by studying the dependence of photoCELIV transients on time delay after the laser pulse as well as dependence on laser intensity. The PhotoCELIV transients recorded in pure PBTDTT-15 film and its photovoltaic blend for various delays after the laser pulse are shown in panels a and b in Figure 6, respectively. It can be seen that the photocurrent maximum decreased with increasing time delay in both devices, indicating significant charge recombination. In pure PBTDTT-15, there was no significant shift in the t_{max} with the time delay, but for the photovoltaic blend the t_{max} slightly shifts to shorter times when the delay time increases. This could be attributed to the fluctuation of internal electric field due to the space charge effects as the photocurrent was nearly 4 times higher than the capacitor current. It is important to note that the PhotoCELIV transients for the photovoltaic blend showed an additional shoulder at longer time, which was absent in the pure film. The PhotoCELIV shoulder at longer time can be attributed to the extraction of holes. It has been shown that the simultaneous measurement of both electron and hole mobility is possible through charge extraction by linearly increasing voltage (CELIV) measurement on polymer heterojunction solar cell based on a copolymer of fluorene and thiophene with highly loaded PCBM blend system (29). It was also noted that the photocharge carriers can be extracted up to 500 μs after the laser pulse, indicating that the lifetime of the charge carriers are significantly long in our material. In the case of MDMO-PPV, the charge extraction was possible only up to 50 μs, indicating that all the carriers recombine within 50 μs (23).

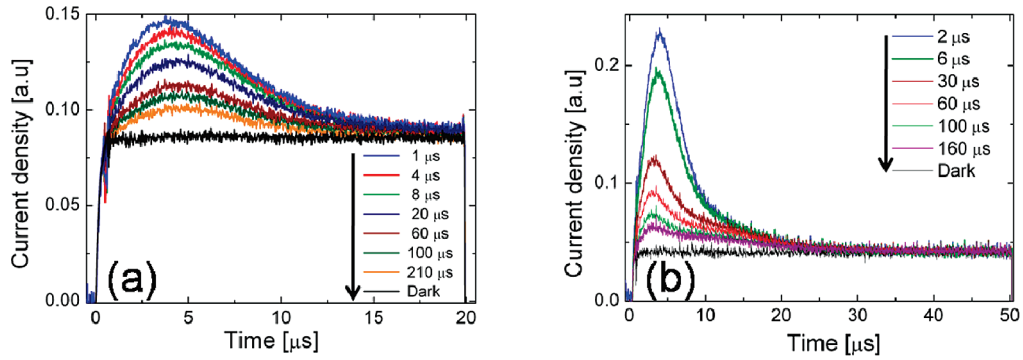

FIGURE 6. PhotoCELIV transients for various time delays from the laser excitation in (a) pure PBTDTT-15 film and (b) PBTDTT-15:$PC_{70}BM$ (1:3) blend film.

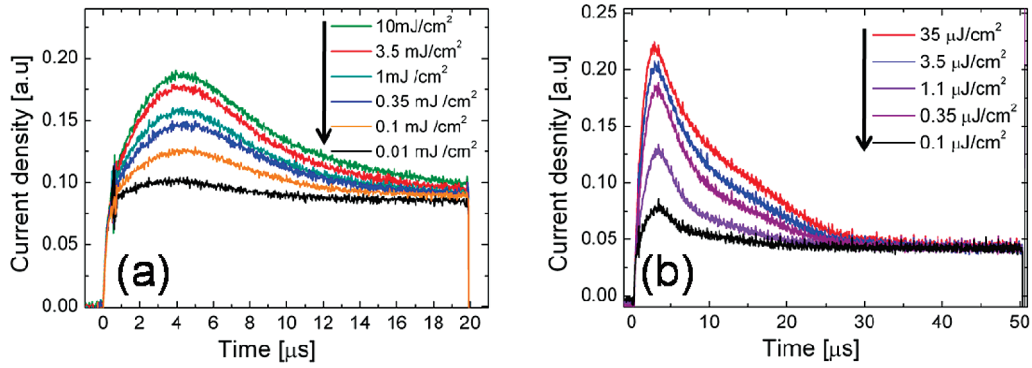

FIGURE 7. PhotoCELIV transients for various laser intensities in (a) pure PBTDTT-15 film and (b) PBTDTT-15:$PC_{70}BM$ (1:3) blend film.

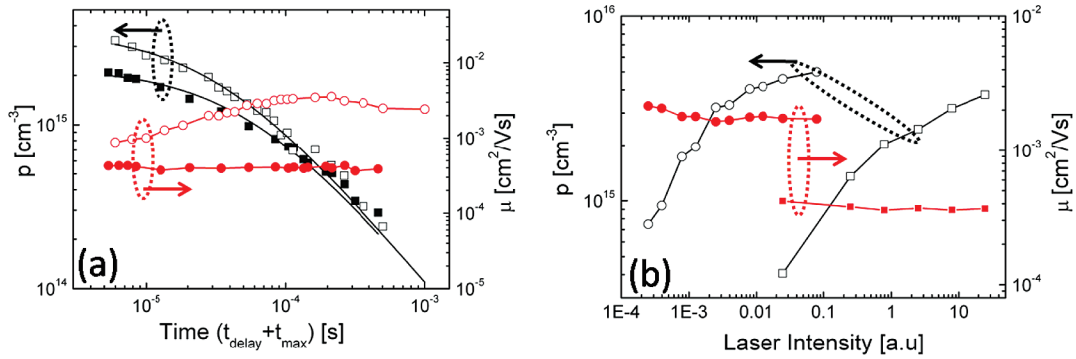

FIGURE 8. (a) Dependence of the number of collected charges (p) and charge mobility (μ) with extraction time in pure PBTDTT-15 and in PBTDTT-15:$PC_{70}BM$; (b) dependence of number of collected charges and charge mobility with laser intensity in PBTDTT-15 and PBTDTT-15:$PC_{70}BM$.

The dependence of photoCELIV transients on laser intensity for the pure PBTDTT-15 film and for the PBTDTT-15:$PC_{70}BM$ (1:3) blend film is shown in panels a and b in Figure 7, respectively. The magnitude of the photoinduced current is increasing with the increase of laser intensity and no saturation of photocurrent was observed for the laser intensities studied. The t_{max} remains almost constant for different laser intensities indicating that the charge mobility is almost independent of number of photoinduced charge carriers. The photoCELIV transients for the photovoltaic blend (Figure 7b) shows an additional shoulder at longer time scale that is more visible at higher laser intensities compared to the photoCELIV transients recorded for lower laser intensities. This additional photoCELIV peak is attributed to the extraction of holes, which is consistent with our TOF photoconductivity studies indicating that the hole mobility is nearly an order of magnitude slower than the electron mobility.

The charge mobility and the number of photogenerated carriers for various time delays after the laser pulse were calculated. The variation of charge mobility and the number of photocharge carriers with extraction time ($t_{max} + t_{del}$) is shown in Figure 8(a). It can be seen that there was no significant change in charge mobility with extraction time, which indicates that the charge mobility is independent of time. It has been shown in reports that the charge mobility in most of the photovoltaic materials are time-dependent, and generally it has been explained by the presence of broad distribution of localized states (23). The time-independent charge mobility obtained in our materials can be explained by the narrow distribution of localized density of states. The observed slight increase in the charge mobility with extraction time for PBTDTT-15:$PC_{70}BM$ photovoltaic blend may be explained by the fluctuation in the electric field due to high density of photocharge carriers. The variation of number of

photocharge carriers with carrier extraction time ($t_{max} + t_{del}$) is also shown in Figure 8a. It is observed that the carrier concentration decreased continuously with time due to recombination. It has been reported that the recombination behavior in disordered semiconductor materials can be well-explained by the bimolecular recombination (30, 31). The simple bimolecular decay can be described as $dp/dt = -\beta p^2$, where β is the bimolecular recombination coefficient and p is the density of photogenerated charge carriers. The solution to the bimolecular decay is given by $p(t) = p_0/(1 + p_0\beta t)$, where p_0 is the initial density of photocharge carriers. The solid line in Figure 8a is a fit to the simple bimolecular decay and the β values were estimated as the model can reasonably fit our experimental data. The estimated β and p_0 for pure PBTDTT-15 film was found to be 9×10^{-12} cm^3/s and 2.2×10^{15} cm^{-3}, whereas in PBTDTT-15:$PC_{70}BM$ blend it was found to be 8.8×10^{-12} cm^3/s and 3.7×10^{15} cm^{-3}, respectively. The obtained β in our materials is almost 1 order of magnitude higher than the value reported for pure regio random poly(3-hexyl thiophene) (30); however, it is in the same range as in poly(dialkoxy *p*-phenylene vinylene) (PPV) (32).

Generally, it has been shown that the bimolecular recombination in organic semiconductors such as PPV (32) and MDMO-PPV:PCBM blends (27) are of Langevin type, where the recombination is diffusion controlled. The simple Langevin type recombination can be described as $\beta_L = e(\mu_e + \mu_h)/\varepsilon\varepsilon_0$, where β_L is Langevin type bimolecular recombination (BR) coefficient, e is the electronic charge (1.602×10^{-19} C), μ_e and μ_h are the electron and hole mobility, ε is the permittivity in free space (8.85×10^{-14} F/cm) and ε_0 is the dielectric constant of the polymer, which is assumed to be ~3. By using the fastest charge mobility of $\sim 3 \times 10^{-3}$ cm^2/(V s) for PBTDTT-15:$PC_{70}BM$ blend, and 4×10^{-4} cm^2/(V s) for pure PBTDTT-15 layer, the calculated β_L is found to be 1.8×10^{-9} cm^3/s and 2.4×10^{-10} cm^3/s, respectively. Therefore, the ratio of β/β_L is found to be $\sim 5 \times 10^{-3}$ and $\sim 4 \times 10^{-2}$ for the PBTDTT-15:$PC_{70}BM$ blend and the pure PBTDTT-15 layer. The observed β/β_L for PBTDTT-15:$PC_{70}BM$ blend shows very good agreement with the value reported for P3HT:PCBM blend, which is around 1×10^{-4}. The obtained results indicate that the bimolecular recombination in our materials was less than the Langevin type bimolecular recombination. The reduced bimolecular recombination can be attributed to a strong phase separated morphology in PBTDTT-15:$PC_{70}BM$ blend. The reduction in bimolecular recombination coefficient has already been observed in highly optimized P3HT:PCBM composites (14).

The dependence of charge mobility and number of photogenerated charge carriers on laser excitation intensity was studied. Figure 8b shows the variation of charge mobility and the number of photogenerated charge carriers with laser intensity. It has been observed that the charge mobility was almost independent of laser intensity, indicating concentration-independent charge mobility characteristics in these materials. The number of photogenerated charge carriers showed linear dependence at lower laser intensities, whereas at high laser intensities, it showed sublinear dependence indicating bimolecular recombination behavior.

4. CONCLUSION

The charge mobility and recombination properties in a new dithienothiophene-based hole-transporting polymer and its blend with $PC_{70}BM$ were investigated using Photo-CELIV and TOF photoconductivity technique. The charge mobility in the bulk heterojunction-based photovoltaic blend: PBTDTT-15:$PC_{70}BM$ (1:3) is in the order of 1×10^{-3} cm^2/(V s), with a promising solar cell power conversion efficiency (PCE) of 3.23%. The hole mobility in the pure polymer is in the order of 1×10^{-4} cm^2/(V s). The carrier dynamics in the photovoltaic blend show reduced non-Langevin type bimolecular recombination of the order of 8.8×10^{-12} cm^3/s at room temperature. The better charge mobility and reduced bimolecular recombination indicates that the PBTDTT-15:$PC_{70}BM$ (1:3) is an efficient photovoltaic blend for polymer solar cell applications.

REFERENCES AND NOTES

(1) Yu, G.; Gao, J.; Hummelen, J. C.; Wudl, F.; Heeger, A. J. *Science* **1995**, *270*, 1789.
(2) Kraft, A.; Grimsdale, A. C.; Holmes, A. B. *Angew. Chem., Int. Ed.* **1998**, *37*, 402.
(3) Liu, J.; Guo, X.; Bu, L.; Xie, Z.; Cheng, Y.; Geng, Y.; Wang, L.; Jing, X.; Wang, F. *Adv. Funct. Mater.* **2007**, *17*, 1917.
(4) Zhang, M.; Tsao, H. N.; Pisula, W.; Yang, C.; Mishra, A. K.; Müllen, K. *J. Am. Chem. Soc.* **2007**, *129*, 3472.
(5) Murphy, R.; Fréchet, M. J. *Chem. Rev.* **2007**, *107*, 1066.
(6) Lee, J. K.; Ma, W. L.; Brabec, C. J.; Yuen, J.; Moon, J. S.; Kim, J. Y.; Lee, K.; Bazan, G. C.; Heeger, A. J. *J. Am. Chem. Soc.* **2008**, *130*, 3619.
(7) Jin, S. H.; Naidu, B. V. K.; Jeon, H. S.; Park, S. M.; Park, J. S.; Kim, S. C.; Lee, J. W.; Gal, Y. S. *Sol. Energy Mater Sol. Cells* **2007**, *91*, 1187.
(8) Kim, Y.; Cook, S.; Tuladhar, S. M.; Choulis, S. A.; Nelson, J.; Durrant, J. R.; Bradley, D. D. C.; Giles, M.; McCulloch, I.; Ha, C. S.; Ree, M. *Nat. Mater.* **2006**, *5*, 197.
(9) Li, G.; Shrotriya, V.; Huang, J.; Yao, Y.; Tommoriarty;Emery, K.; Yang, Y. *Nat. Mater.* **2005**, *4*, 864.
(10) Gong, C.; Song, Q. L.; Yang, H. B.; Li, J.; Li, C. M. *Sol. Energy Mater. Sol. Cells* **2009**, *93*, 1928.
(11) Liang, Y. Y.; Wu, Y.; Feng, D. Q.; Tsai, S. T.; Son, H. J.; Li, G.; Yu, L. P. *J. Am. Chem. Soc.* **2009**, *131* (1), 56–57.
(12) Park, S. H.; Roy, A.; Beaupre, S.; Cho, S.; Coates, N.; Moon, J. S.; Moses, D.; Leclerc, M.; Lee, K. H.; Heeger, A. J. *Nat. Photonics* **2009**, *3*, 297.
(13) Kim, J. Y.; Lee, K. H.; Coates, N. E.; Moses, D.; Nguyen, T. Q.; Dante, M.; Heeger, A. J. *Science* **2007**, *317*, 222.
(14) Pivrikas, A.; Sariciftci, N. S.; Jus°ka, G.; Ošterbacka, R. *Prog. Photovolt: Res. Appl.* **2007**, *15*, 677–696.
(15) Mozer, A. J.; Sariciftci, N. S.; Lutsen, L.; Vanderzande, D.; Osterbacka, R.; Westerling, M.; Juska, G. *Appl. Phys. Lett.* **2005**, *86*, 112104.
(16) Zhang, S. M.; He, C.; Liu, Y.; Zhan, X. W.; Chen, J. W. *Polymer* **2009**, *50*, 3595.
(17) Morrison, J. J.; Murray, M. M.; Li, X. C.; Holmes, A. B.; Morratti, S. C.; Friend, R. H.; Sirringhaus, H. *Synth. Met.* **1999**, *102*, 987.
(18) Iosip, M. D.; Destri, S.; Pasini, M.; Porzio, W.; Pernstitch, K. P.; Batlogg, B. *Synth. Met.* **2004**, *146*, 251.
(19) Luzzati, S.; Basso, M.; Catellani, M.; Brabec, C. J.; Gebeyehu, D.; Sariciftci, N. S. *Thin Solid Films* **2002**, *403*, 52.
(20) Millefiorini, S.; Kozma, E.; Catellani, M.; Luzzati, S. *Thin Solid Films* **2008**, *516*, 7205.
(21) Kim, K. H.; Kim, D. C.; Cho, M. J.; Choi, D. H. *Macromol. Res.* **2009**, *17*, 549.
(22) Juska, G.; Arlauskas, K.; Viliunas, M.; Kocka, J. *Phys. Rev. Lett.* **2000**, *84*, 4946–4949.
(23) Denler, G.; Mozer, A. J.; Juska, G.; Pivrikas, A.; Osterbacka, R.; Fuchsbaur, A.; Sariciftci, N. S. *Org. Electron.* **2006**, *7*, 229–223.

(24) Tang, W.; Vijila, C.; Liu, M.; Chen, Z.; Ke, L. *ACS: Appl. Mater. Interfaces* **2009**, *1*, 1467–1473.
(25) Chellappan, V.; Almantas, P.; Huang, C.; Chen, Z.-K.; Ronald, O.; Chua, S. J. *Org. Electron.* **2007**, *8*, 8–13.
(26) Chellappan, V.; Bavani, B.; Huang, C.; Chen, Z.-K.; Zhen, C.; Auch, M. D. J.; Chua, S. J. *Chem. Phys. Lett.* **2005**, *414*, 393–397.
(27) Mozer, A. J.; Sariciftci, N. S.; Pivrikas, A.; Österbacka, R.; Juška, G.; Brassat, L.; Bässler, H. *Phys. Rev.* **2005**, *71*, 035214–9.
(28) Choulis, S. A.; Nelson, J.; Kim, Y.; Poplavskyy, D.; Kreouzis, T.; Durrant, J. R.; Bradley, D. D. C. *Appl. Phys. Lett.* **2003**, *83*, 3812–3814.
(29) Andersson, L. M.; Zhang, F. L.; Inganas, O. *Appl. Phys. Lett.* **2006**, *89*, 142111–3.
(30) Juska, G.; Viliunas, M.; Arlauskas, K.; Stuchlik, J.; Kocka, J. *Phys. Status Solidi A* **1999**, *171*, 539–547.
(31) Osterbacka, R.; Pivrikas, A.; Juska, G.; Genevicius, K.; Arlauskas, K.; Stubb, H. *Curr. Appl. Phys.* **2004**, *4*, 534–538.
(32) Blom, P. W. M.; de Jong, M. J. M.; Breedijk, S. *Appl. Phys. Lett.* **1997**, *71*, 930–932.

AM100078G